



HAL
open science

Mechanisms for Lasing with Cold Atoms as the Gain Medium

William Guerin, Franck Michaud, Robin Kaiser

► **To cite this version:**

William Guerin, Franck Michaud, Robin Kaiser. Mechanisms for Lasing with Cold Atoms as the Gain Medium. 2008. hal-00268718v2

HAL Id: hal-00268718

<https://hal.science/hal-00268718v2>

Preprint submitted on 27 May 2008 (v2), last revised 29 Aug 2008 (v3)

HAL is a multi-disciplinary open access archive for the deposit and dissemination of scientific research documents, whether they are published or not. The documents may come from teaching and research institutions in France or abroad, or from public or private research centers.

L'archive ouverte pluridisciplinaire **HAL**, est destinée au dépôt et à la diffusion de documents scientifiques de niveau recherche, publiés ou non, émanant des établissements d'enseignement et de recherche français ou étrangers, des laboratoires publics ou privés.

Mechanisms for Lasing with Cold Atoms as the Gain Medium

William Guerin, Franck Michaud, and Robin Kaiser*

*Institut Non Linéaire de Nice, CNRS and Université de Nice Sophia-Antipolis,
1361 route des Lucioles, 06560 Valbonne, France.*

(Dated: May 27, 2008)

We realize a laser with a cloud of cold rubidium atoms as gain medium, placed in a low-finesse cavity. Three different regimes of laser emission are observed corresponding respectively to Mollow, Raman and Four Wave Mixing mechanisms. We measure an output power of up to 300 μ W and present the main properties of these different lasers in each regime.

PACS numbers: 33.20.Fb, 37.30.+i, 42.55.Ye, 42.55.Zz, 42.65.Hw

Since the Letokhov's seminal paper [1], random lasers have received increasing interest in the past decade. Random lasing occurs when the optical feedback due to multiple scattering in the gain medium itself is sufficiently strong to reach the lasing threshold. So far, it has been observed in a variety of systems (see [2] for a review) but many open questions remain to be investigated, for which better characterized samples would be highly valuable. A cloud of cold atoms could provide a promising alternative medium to study random lasing, allowing for a detailed understanding of the microscopic phenomena and a precise control of essential parameters such as particle density and scattering cross section. These properties have been exploited to study radiation trapping [3] and coherent backscattering of light [4] in large clouds of cold atoms. As many different gain mechanisms have been observed with cold atoms, combining multiple scattering and gain in cold atomic clouds seems a promising path towards the realization of a new random laser. Besides the realization of a random laser, cold atoms might allow to study additional features, such as the transition from superfluorescence to amplified spontaneous emission [5] in a multiple scattering regime. One preliminary step along this research lines is to use a standard cavity to trigger laser oscillation with cold atoms as gain medium. Such a laser may also be an interesting tool for quantum optics, as one can take advantage of the nonlinear response of the atoms to explore non classical correlations or obtain squeezing [6].

In this letter, we present the realization of a cold-atom laser, that can rely on three different gain mechanisms, depending on the pumping scheme. By pumping near resonance, Mollow gain [7, 8] is the dominant process and gives rise to a laser oscillation, whose spectrum is large (of the order of the atomic natural linewidth), whereas by pumping further from resonance, Raman gain between Zeeman sublevels [9] gives rise to a weaker, spectrally sharper laser [10]. At last, by using two counter-propagating pump beams, degenerate four-wave mixing (FWM) [11, 12] produces a laser with a power up to 300 μ W. By adjusting the atom-laser detuning or the pump geometry, we can continuously tune the laser from one regime to another.

Our experiment uses a cloud of cold ^{85}Rb atoms confined in a vapor-loaded Magneto-Optical Trap (MOT) produced by six large independent trapping beams, allowing the trapping of up to 10^{10} atoms at a density of 10^{10} at/cm³, corresponding to an on-resonance optical thickness of about 10. A linear cavity, formed by two mirrors (a coupling-mirror with curvature $RC1 = 1$ m, reflection coefficient $R1 = 0.95$ and plane end-mirror with reflection coefficient $R2 \approx 0.995$) separated by a distance $L = 0.8$ m is placed outside the vacuum chamber, yielding a large round trip loss $\mathcal{L} = 32\%$ with a correspondingly low finesse $\mathcal{F} = 16$. The waist of the fundamental mode of the cavity at the MOT location is $w_{\text{cav}} \approx 500$ μm . To add gain to our system, we use either one or two counter-propagating pump beams, denoted F (forward) and B (backward), produced from the same laser with a waist $w_{\text{pump}} = 2.6$ mm, with linear parallel polarizations and a total available power of $P = 80$ mW, corresponding to a maximum pump intensity of $I = 2P/(\pi w_{\text{pump}}^2) \approx 750$ mW/cm². The pump is tuned near the $F = 3 \rightarrow F' = 4$ cycling transition of the $D2$ line of ^{85}Rb (frequency ω_A , wavelength $\lambda = 780$ nm, natural linewidth $\Gamma/2\pi = 5.9$ MHz), with an adjustable detuning $\Delta = \omega_{F,B} - \omega_A$ and has an incident angle of $\approx 20^\circ$ with the cavity axis. An additional beam P is used as a local oscillator to monitor the spectrum of the laser or as a weak probe to measure single-pass gain (insets of Figs. 2-4) with a propagation axis making an angle with the cavity axis smaller than 10° . Its frequency ω_P can be swept around the pump frequency with a detuning $\delta = \omega_P - \omega_{F,B}$. Both lasers, pump and probe, are obtained by injection-locking of semiconductor lasers from a common master laser, which allows to resolve narrow spectral features. All our experiments are time-pulsed with a cycling time of 30 ms. The trapping period lasts 29 ms, followed by a dark period of 1 ms, when the MOT trapping beams and magnetic field are switched off. In order to avoid optical pumping into the dark hyperfine $F = 2$ ground state, a repumping laser is kept on all time. Lasing or pump-probe spectroscopy are performed during the dark phase, short enough to avoid expansion of the atomic cloud. Data acquisitions are the result of an average of typically 1000 cycles.

As in a conventional laser, lasing occurs if gain exceeds losses in the cavity, which can be observed as strong directional light emission from the cavity. As we will discuss in detail below, we are able to produce lasing with cold atoms as gain medium using three different gain mechanisms: Mollow gain, Raman gain and Four Wave Mixing (FWM). We can control the different mechanisms by the pump geometry and the pump detuning Δ (see Table I). Mollow and Raman gain mechanisms only require a single pump beam (F), whereas FWM only occurs when both pump beams F and B are present and carefully aligned. With a single pump beam, we find Mollow gain to be dominating close to the atomic resonance, whereas Raman gain is more important for detunings larger than $|\Delta| \approx 4\Gamma$. Furthermore, the different gain mechanisms lead to distinct polarizations. Mollow gain generates a lasing mode with a polarization parallel to the pump polarization, because the Mollow amplification is maximum for a field aligned with the driven atomic dipole [7]. On the contrary, different polarizations between the pumping and the amplified waves are necessary to induce a Raman transition between two Zeeman substates: the polarization of the Raman laser is thus orthogonal to the pump polarization. Lastly, the FWM laser has a more complex polarization behaviour, as it is orthogonal for red-, and parallel for blue-detuned pumps. We have checked that for any pump detuning or probe power, the weak-probe FWM reflectivity is stronger for orthogonal probe polarization, as expected from previous experiments and models [13]. We speculate that pump-induced mechanical effects [14] or more complex collective coupling between the atoms and the cavity [15] might be the origin of this polarization behavior.

In Fig. 1 we show spatial (transverse) patterns of these lasers, observed by imaging the beam onto a CCD camera. Without any spatial filtering in the cavity, the different lasers (Mollow, Raman and FWM) yield distinct transverse patterns. In Fig. 1(b) (resp. 1(c)) we show the transverse pattern obtained with a Mollow (resp. Raman) laser. We note that the Mollow laser typically produces transverse patterns with radial symmetries well described by Laguerre-Gauss modes, whereas the modes of the Raman laser are rather Hermite-Gauss modes. The origin of such radial or cartesian symmetry may arise from the different polarization of those two lasers: the radial symmetry is preserved for the Mollow laser polarization and is broken for the Raman laser one, probably

pump beam(s)	$\Delta < -4\Gamma$	$-4\Gamma < \Delta < +4\Gamma$	$\Delta > +4\Gamma$
F	Raman (\perp)	Mollow ($//$)	Raman (\perp)
F+B	FWM (\perp)	Mollow ($//$)	FWM ($//$)

TABLE I: Different regimes of cold-atom laser versus pump detuning. The polarization of the lasers are either parallel ($//$) or orthogonal (\perp) to the polarization of the pump beams.

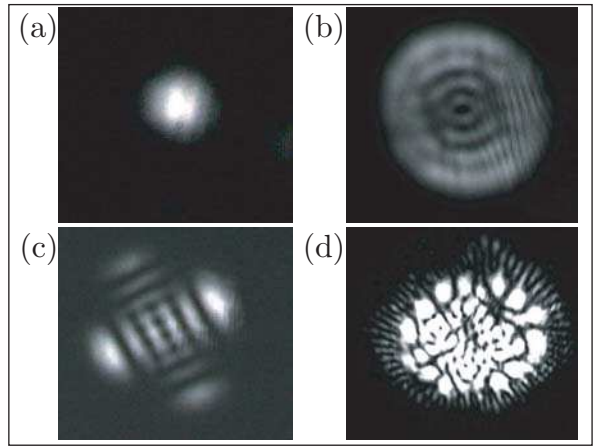


FIG. 1: Transverse modes of the different cold-atom lasers. (a) Gaussian TEM_{00} mode, obtained by inserting a small diaphragm near the waist of the cavity. Typical modes of: (b) the Mollow laser, (c) the Raman laser, and (d) the four-wave mixing laser respectively.

due to slightly different losses in the cavity. Fig. 1(d) shows the transverse pattern of the FWM laser. As phase conjugation mechanisms are at work in such a laser, any transverse mode can easily cross the lasing threshold and complex lasing patterns are produced [16].

We now turn to a more detailed description of the gain mechanisms of the different lasers. The quantitative understanding of their behavior needs to take into account effects such as pump geometry and parameters (intensity, detuning), gain spectra, gain saturation, mechanical effects induced by the pump beam(s).

Let us first discuss the Mollow laser. Amplification of a weak probe beam can happen when a two-level atom is excited by one strong pump beam [7, 8]. The corresponding single-pass gain is written as

$$g_M = e^{-b_0 f_M(\Omega, \Delta, \delta)}, \quad (1)$$

where b_0 is the on-resonance optical thickness (without pump) of the cold-atom cloud. The expression of $f_M(\Omega, \Delta, \delta)$ can be obtained from Optical Bloch Equations [7]:

$$f_M(\Omega, \Delta, \delta) = \frac{\Gamma}{2} \frac{|z|^2}{|z|^2 + \Omega^2/2} \times \Re \left[\frac{(\Gamma + i\delta)(z + i\delta) - i\Omega^2\delta/(2z)}{(\Gamma + i\delta)(z + i\delta)(z^* + i\delta) + \Omega^2(\Gamma/2 + i\delta)} \right], \quad (2)$$

where $z = \Gamma/2 - i\Delta$ and Ω is the Rabi frequency of the atom-pump coupling, related to the pump intensity I by $\Omega^2 = \mathcal{C}^2 \Gamma^2 I / (2I_{\text{sat}})$ ($I_{\text{sat}} = 1.6 \text{ mW/cm}^2$ is the saturation intensity and \mathcal{C} is the averaged Clebsch-Gordan coefficient of the $F = 3 \rightarrow F' = 4$ transition for a linear polarization). In our setup we observe single-pass gain higher than 50%, with a large gain curve (width $> \Gamma$). The shape of the transmission spectrum (inset of Fig.

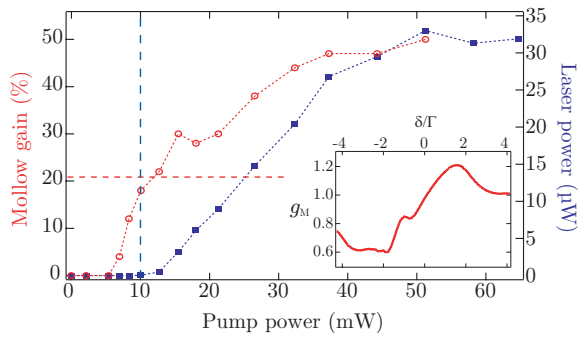


FIG. 2: Laser power (squares) and Mollow gain (open circles) versus pump power, with $b_0 = 11$ and $\Delta = +\Gamma$. Lasing threshold (vertical dashed line) is expected to appear with a gain of about 21% (horizontal dashed line), in good agreement with the experimental data. Inset: typical weak-probe transmission spectrum.

2) is consistent with Eqs. (1-2). From Eq. (2) we can also predict the maximum gain in respect to the pump parameters Ω , Δ . We observe good agreement between the behavior of the laser power and of the function f_M when varying Δ : the maximum gain and laser power are achieved for $|\Delta| \sim 2\Gamma$ (the exact value depends on Ω) and $\Delta = 0$ is a local minimum. However, we measured a lower maximum gain than predicted by Eqs. (1-2). This is due to gain-saturation induced by re-scattering of spontaneous emission inside the atomic cloud [17].

As shown in Fig. 2 (squares), we observe a Mollow laser emission with an output intensity reaching $35 \mu\text{W}$. Taking into account the round-trip losses \mathcal{L} , the condition for laser oscillation is $g_M^2(1 - \mathcal{L}) > 1$. This corresponds to a gain at threshold of $g_M = 1.21$ (horizontal line in Fig. 2), in good agreement with the observation.

When the pump frequency is detuned farther away from the atomic resonance, Raman gain becomes dominant. Raman gain relies on the pump-induced population inversion among the different light-shifted m_F Zeeman sublevels of the $F = 3$ hyperfine level [9, 18]. Single-pass Raman gain of a weak probe can be written as:

$$g_R = e^{-b_0 f_R(\Omega, \Delta, \delta)}, \quad (3)$$

with the function f_R given by

$$f_R = -\frac{\Omega^2}{\Delta^2} \left(\frac{A_1}{(\delta + \delta_R)^2 + \gamma^2/4} - \frac{A_2}{(\delta - \delta_R)^2 + \gamma^2/4} \right), \quad (4)$$

where $A_{1,2}$ are the respective weights of the amplification and absorption, δ_R is the frequency difference between the Zeeman sublevels and γ is the width of the Raman resonance [18]. We have observed the laser spectrum with a beat-note experiment, and we have checked that its frequency corresponds to the maximum gain and is related to the differential pump-induced light-shift δ_R of the different Zeeman sublevels. The width of the Raman resonance γ is related to the elastic scattering rate of

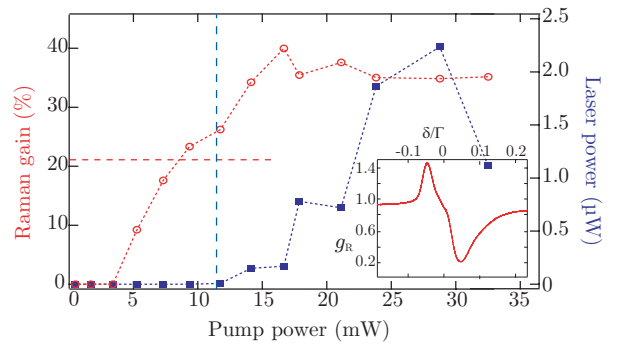


FIG. 3: Laser power (squares) and Raman gain (open circles) versus pump power, with $b_0 = 10$ and $\Delta = -7\Gamma$. Lasing threshold (vertical dashed line) is expected to appear with a gain of about 21% (horizontal dashed line), in good agreement with the experimental data. Inset: typical weak-probe transmission spectrum.

the pump photons and is much lower than Γ , due to the strong detuning Δ . The result is thus a much narrower gain spectrum than in the previous case (inset of Fig. 3). This leads to an important practical limitation of the single-pumped Raman laser: atoms are pushed by the pump beam, acquiring a velocity v , and the subsequent Doppler shift becomes quickly larger than the width of the gain spectrum. As a consequence, the gain in the cold-atom cloud is no longer the same for a wave copropagating with the pump beam (F) and the wave running in the counterpropagating direction. For the copropagating direction, the relative Doppler shift is negligible, whereas for the counterpropagating wave, a Doppler shift of $\sim 2\omega_\Delta v/c$, larger than the width of the gain spectrum, leads to a suppression of the corresponding gain. As a consequence, emission of our Raman laser stops after $\approx 20 \mu\text{s}$ [19].

In Fig. 3 we plot the output power of the Raman laser as a function of pump power. A comparison with the single-pass gain g_R is again in good agreement for the threshold condition $g_R^2(1 - \mathcal{L}) > 1$: for Raman gain above 21% laser emission occurs. As shown in Fig. 3 (squares), the output power of the Raman laser emission ($\approx 2 \mu\text{W}$) is much lower than the Mollow laser one. This lower output power might arise from a lower saturation intensity for Raman gain [20]. Nevertheless, with a weak signal, the Raman gain can be as high as $g_R = 2$ [20].

We have observed another lasing mechanism when a balanced pumping scheme using two counterpropagating pump beams F and B is used. In this configuration FWM appears [11, 12]. The creation of photons in a reflected wave, resulting from a phase conjugation process, can also be considered as a gain mechanism. This is reminiscent of optical parametric oscillation (OPO) where signal and idler photons are created under a phase matching condition. In the inset of Fig. 4 we show the FWM signal R_c (expressed as the reflection normalized to the

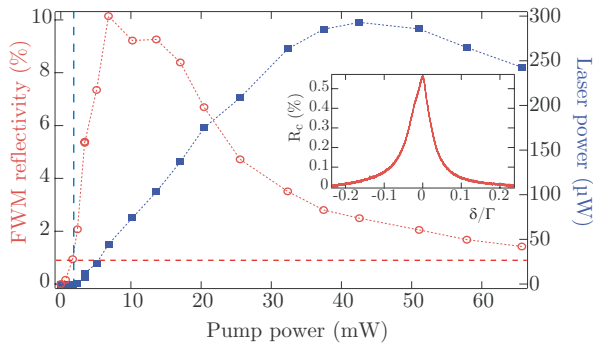


FIG. 4: Laser power (squares) and phase-conjugate reflectivity due to four-wave mixing (open circles) versus pump power, with $b_0 = 10$ and $\Delta = -8\Gamma$. Lasing threshold (vertical dashed line) is expected for a reflectivity around 1% (Eq. 5, horizontal dashed line), in good agreement with the experimental data. Inset: example of a weak-probe reflectivity spectrum.

incident probe power) illustrating the narrow spectrum of this phase conjugation signal. As expected, the maximum gain corresponds to the degenerate case $\delta = 0$ [13]. Thanks to constructive interference between transmitted and reflected waves, this mechanism produces huge double-pass gain with cold atoms [20] and it is thus an efficient mechanism to trigger laser oscillations [21]. Due to these interference effects, the threshold for laser oscillation is very different from the previous cases [20, 21], and is given by

$$R_c > \left(\frac{1 - \sqrt{\tilde{R}}}{1 + \sqrt{\tilde{R}}} \right)^2 = 0.9\%, \quad (5)$$

where $\tilde{R} = 1 - \mathcal{L}$. In Fig. 4, we see that this criterium (indicated by the horizontal line) is well respected for the threshold of our laser. The output power of this laser is quite strong (300 μW), with an energy conversion efficiency of 0.75% in this case. We note that as two pump beams are used in this situation, the mechanical effects based on radiation pressure will be negligible and lasing can be sustained for a long time. However atomic bunching, due to the dipole force, can occur, thus changing the effective pump intensity interacting with the atoms [14].

In conclusion, we presented in this letter three types of laser using a sample of cold atoms as gain medium. Three different gain mechanisms were demonstrated as being efficient enough to allow lasing, even with a low finesse cavity. Comparison between Mollow and Raman laser shows that the latter has a significantly lower power, although their gain are of the same order of magnitude. These two mechanisms can produce high gain at frequencies slightly detuned from the pump, allowing to distinguish between stimulated photons from the laser mode and scattered photons from the pump beam. Thus, they seem to be good candidates for the search of random lasing in cold atoms, and the combination of these gains with multiple

scattering will be the subject of further investigations. In addition, the ability to continuously tune from a Mollow to a Raman laser (by changing the pump detuning), may allow to study the transformation of transverse patterns from Laguerre-Gauss to Hermite-Gauss modes [22]. The FWM laser is the most efficient in terms of power, and it should be possible to study its noise spectrum down to the shot noise level. This laser has many analogies to an OPO and seems to be a good candidate to explore non classical features of light. Thanks to the strong correlation between the transmitted and conjugated waves, it can for instance be used to produce twin beams [23, 24]. Lastly, the coupling between the cavity mode and the atomic internal and external degrees of freedom, may also reveal interesting dynamics [15, 25].

The authors would like to thank G.-L. Gattobigio for his help at the early stages of the experiment. This work is supported by CNRS, PACA Region and the project ANR-06-BLAN-0096. F.M. is funded by DGA.

* Electronic address: Robin.Kaiser@inln.cnrs.fr

- [1] V. S. Letokhov, *Sov. Phys. J. Exp. Theoret. Phys.* **26**, 835 (1968).
- [2] H. Cao, *Waves Random Media* **13**, R1 (2003).
- [3] G. Labeyrie, R. Kaiser, and D. Delande, *Appl. Phys. B* **81**, 1001 (2005).
- [4] G. Labeyrie *et al.*, *Phys. Rev. Lett.* **83**, 5266 (1999).
- [5] M. S. Malcuit *et al.*, *Phys. Rev. Lett.* **59**, 1189 (1987).
- [6] R. E. Slusher *et al.*, *Phys. Rev. Lett.* **55**, 2409 (1985).
- [7] B. R. Mollow, *Phys. Rev. A* **5**, 2217 (1972).
- [8] F. Y. Wu *et al.*, *Phys. Rev. Lett.* **38**, 1077 (1977).
- [9] D. Grison *et al.*, *Europhys. Lett.* **15**, 149 (1991); J. W. R. Tabosa *et al.*, *Phys. Rev. Lett.* **66**, 3245 (1991).
- [10] L. Hilico, C. Fabre, and E. Giacobino, *Europhys. Lett.* **18**, 685 (1992).
- [11] A. Yariv and D. M. Pepper, *Opt. Lett.* **1**, 16 (1977).
- [12] R. L. Abrams and R. C. Lind, *Opt. Lett.* **2**, 94 (1978), *Opt. Lett.* **3**, 205 (1978).
- [13] A. Lezama, G. C. Cardoso and J. W. R. Tabosa, *Phys. Rev. A* **63**, 013805 (2000).
- [14] G.-L. Gattobigio *et al.*, *Phys. Rev. A* **74**, 043407 (2006).
- [15] D. Nagy *et al.*, *Europhys. Lett.* **74**, 254 (2006).
- [16] R. C. Lind and D. G. Steel, *Opt. Lett.* **6**, 554 (1981).
- [17] L. Khaykovich, N. Friedman and N. Davidson, *Eur. Phys. J. D* **7**, 467 (1999).
- [18] T. M. Brzozowski *et al.*, *Phys. Rev. A* **71**, 013401 (2005).
- [19] Note that the single-pumped Mollow laser suffers also from mechanical effects of the pump (atoms are pushed away), but at a time scale typically larger than 100 μs .
- [20] F. Michaud *et al.*, *J. Opt. Soc. Am. B* **24**, A40 (2007).
- [21] M. Pinard, D. Grandclement, and G. Grynberg, *Europhys. Lett.* **2**, 755 (1986).
- [22] E. G. Abramochkin and V. G. Volostnikov, *J. Opt. A: Pure Appl. Opt.* **6**, S157 (2004).
- [23] M. Vallet, M. Pinard, and G. Grynberg, *Europhys. Lett.* **11**, 739 (1990).
- [24] C. F. McCormick *et al.*, *Opt. Lett.* **32**, 178 (2007).
- [25] D. Kruse *et al.*, *Phys. Rev. Lett.* **91**, 183601 (2003).